

Nanoscale

Accepted Manuscript



This is an *Accepted Manuscript*, which has been through the Royal Society of Chemistry peer review process and has been accepted for publication.

Accepted Manuscripts are published online shortly after acceptance, before technical editing, formatting and proof reading. Using this free service, authors can make their results available to the community, in citable form, before we publish the edited article. We will replace this *Accepted Manuscript* with the edited and formatted *Advance Article* as soon as it is available.

You can find more information about *Accepted Manuscripts* in the [Information for Authors](#).

Please note that technical editing may introduce minor changes to the text and/or graphics, which may alter content. The journal's standard [Terms & Conditions](#) and the [Ethical guidelines](#) still apply. In no event shall the Royal Society of Chemistry be held responsible for any errors or omissions in this *Accepted Manuscript* or any consequences arising from the use of any information it contains.

ARTICLE

Compact, all-optical, THz wave generator based on self modulation in a slab photonic crystal waveguide with a single sub-nanometer graphene layer

Cite this: DOI: 10.1039/x0xx00000x

Received 00th May 2015,
Accepted 00th May 2015

DOI: 10.1039/x0xx00000x

www.rsc.org/

R. Asadi,^a Z. Ouyang^a and M. M. Mohammad^b,

We design a compact, all-optical THz wave generator based on self modulation in a 1-D slab photonic crystal (PhC) waveguide with a single sub-nanometer graphene layer by using enhanced nonlinearity of graphene. It has been shown that at the bandgap edge of higher bands of 1-D slab PhC, through only one sub-nanometer graphene layer we can obtain a micro, high modulation factor (about 0.98 percent), self intensity modulator at high frequency (about 0.6 THz) and low threshold intensity (about 15 MW per square centimeter), and further a compact, all-optical THz wave generator by integrating the self modulator with a THz photodiode or photonic mixer. Such a THz source is expected to have a relatively high efficiency compared with conventional ones based on optical methods. The proposed THz source can find wide applications in THz science and technology, e.g., in THz imaging, THz sensors and detectors, THz communication systems, and THz optical integrated logic circuits.

Introduction

In recent years, THz science and technology are attracting great attentions in imaging [1], sensing [2] and communications [3, 4], as THz rays are damage free to materials, have high ability in penetrating many materials including cloths and plastics, and are rich in frequency resources. For all THz applications, THz sources are the basic devices. Generally, the following ways are used to provide THz sources: (1) nonlinear optical frequency difference [5, 6]; (2) nonlinear parametric process [7, 8]; (3) optical rectification [9]; (4) quantum cascade THz laser [10-13]; (5) frequency multiplication [14, 15]; (6) Gunn generator [16, 17]; (7) THz free-electron lasers [18]; (8) photomixer [19]; (9) traveling-wave photodiodes [20]. At present, however, achieving compact, efficient, economic THz sources remains a challenge to scientists and engineers [20-23]. In case (1) the efficiency and power are very low especially for CW operations, the system is bulky, and the technical difficulty is high as two frequency-locked, mode-matched, same-polarization-state optical beams of high power are required; in case (2), the efficiency is also low because idle waves are required in the parametric process and the system is bulk as well because a complicated optical amplifier is required; in case (3) the efficiency is very low because a lot of unwanted frequencies are generated and the system is large because a fs pulse laser is

required, in case (4) a very low operation temperature is required and in the cases (5) – (6), the efficiency is also quite low and the frequency range is limited because the response of electronic devices in THz bands are very poor; while in case (7), the system is generally very large.

Finally, in case (8) and (9) that are mainly used for CW operations, heterodyne method and THz beat frequency of two frequency-locked laser beams with two different frequencies are used, resulting complicated system, technical difficulties and high cost. Also in these methods, tuning of the THz beat frequency is to be realized by tuning the laser frequency, which is generally not so easy.

To overcome the difficulties and complexity in the cases (8) and (9), in this paper we report a novel THz source with a compact size based on self-modulation of an optical wave in a slab photonic crystal waveguide with a single sub-nanometer graphene layer. In addition, we will show that in this method tuning of the THz frequency can be obtained by changing the laser intensity in addition to changing the wavelength of the laser beam. This provides a novel, more easy way for tuning the output frequency of THz wave generators.

Graphene, a new nonlinear material with high Kerr nonlinearity having a much easier fabrication process than conventional nonlinear materials, opened a new way for designing nonlinear optical devices with better performance. However its relatively

high absorption coefficient ($\sim 2.3\%$ for each layer) sets a high limitation for its applications in nonlinear optical devices. Furthermore, graphene is extremely thin in thickness (~ 0.34 nm), which forces one to use a large number of graphene layers to obtain required nonlinearity (thus higher absorption) or a high intensity pump beam to get sensible Kerr nonlinear effects averaged in a certain volume of material. These limitations lead to that until now the high nonlinearity of graphene has been mainly utilized for saturable absorption applications such as mode locking and Q switching for lasers [24-26]. However, in our previous report [27], we have shown that using a single layer of graphene in sub-nanometer thickness as a nonlinear material inside 1-D PhCs is sufficient to overcome the mentioned limitations, so that all optical sensitive phase shifters based on sharp phase changing around the Fano resonance in a slab PhC could be designed.

In addition to its high nonlinearity, another interesting feature of graphene is its fast nonlinear response which is due to the fast (~ 100 fs) intra band transitions [28]. Here we will show that using light propagation inside 1-D slab PhCs with a single layer of graphene at frequencies near the bandgap edges of high normalized frequencies ($f > 1$), we can obtain suitable high nonlinearity and short response time for low threshold and high modulation factor all optical self intensity modulators.

Using PhC modes with higher quality factors helps to increase the light enhancement factor and thus reducing the threshold pump intensity required. But on the other hand, it can increase the response time of the PhC and can limit the modulation frequency. Thus, to achieve high frequency modulation with low threshold intensity in THz bands, it is necessary to choose modes with suitable quality factors. We will show in this study that higher bands of 1-D slab PhCs are good choices for this purpose. The advantage of using 1-D slab PhC is its easier fabrication process through simpler mask for micro lithography without requiring line defects as a waveguide. In addition, using higher normalized frequencies leads to larger lattice period and thus much easier fabrication process. However, higher normalized frequencies (above light line) lead to out of plane loss, but as we will show, this loss is not so high in small PhCs. Therefore, one can utilize these frequencies to design optical devices with relatively low loss.

As a result, we can design a compact, all-optical THz wave generator by integrating the self-modulator with a THz photodiode or a photonic mixer.

Such a THz source is expected to have a relatively high efficiency compared with conventional ones based on nonlinear optical processes because the nonlinearity of graphene is high and enhanced in the structure proposed. It is also very compact with less complexity and easier implementation especially compared with the conventional heterodyne method which applies two frequency-locked, mode-matched, same-polarization-state lasers with different frequencies because in our method only one laser beam is required in the system and its size is in micrometer order. The proposed THz source can find wide applications in THz science and technology, e.g., in THz imaging, THz sensors and detectors, THz communication systems, and THz optical integrated logic circuits.

Physical model of the THz wave generator proposed

The schematic of the THz wave generator proposed is shown in Fig. 1. The structure includes a 1-D silicon (Si) PhC of 5 periods with a single layer of graphene in sub-nanometer thickness in the middle cell of the PhC. The substrate is SiO_2 and the PhC is between two Si waveguides. The filling factor ($F = w/a$) of Si in the PhC is 0.9 and the thickness of Si layer is $h = 0.5a$, where a is the period of the PhC that is selected by considering the operation wavelength corresponds to the communication wavelength of $\lambda = 1550$ nm. As we will show in the next sections, for our purpose the suitable normalized frequency is about 1.138, so we will have $a \approx 1760$ nm. We consider an equivalent composite of Gr and Si with $d = 0.02a$ at $y = 0.5h$. The horizontal width of the composite layer is the same as that of the silicon layer in the PhC unit cell. For the illumination, we consider a light polarized in z-direction inputted from the left-hand-side waveguide, as shown in Fig. 1. The self modulated wave will be converted to THz wave through the PD or PM in Fig. 1. Considering the conversion process in the PD or PM is a standard one, therefore, in the following we focus on the analysis and demonstration of self modulation in the structure.

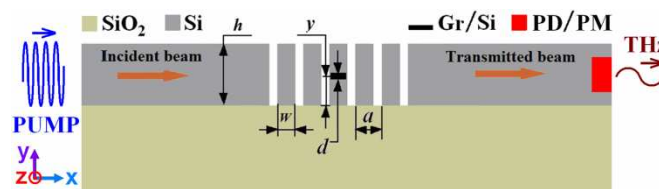


Fig. 1. Schematic of the THz wave generator. It consists of a one-dimensional (1-D) slab PhC, which is illuminated from the waveguide at the left side of the PhC, a layer of graphene (Gr) in sub-nanometer thickness, and a photodiode (PD) or a photonic mixer (PM). An infrared wave with a wavelength of 1550 nm is inputted from the left-hand side and self modulated in the structure. Finally, the self-modulated wave is converted into THz wave by the PD or PM and radiated out from the right-hand side.

We mention that there is an important difference between the above structure and that in our previous work [27]: the input wave is from the left-hand side of the waveguide in the present configuration, while the input wave comes from the top side of the waveguide, i.e., there is no vertical to horizontal coupling of waves as that in the previous work. Moreover, the present structure operates on the principle of self amplitude modulation, while the previous one is based on nonlinear phase modulation.

Calculation method

In order to determine the suitable normalized frequency, we first calculate the linear transmission spectrum (versus normalized frequency). For calculation of transmission coefficient, we use an incident beam with a Gaussian profile with its full width at half maximum (FWHM) equals to the half of the height of the waveguide, we calculate the transmission in a standard definition as that in our previous report [27], and then we perform nonlinear FDTD simulation to calculate the change of PhC transmission for different intensities of the pump beam at the selected normalized frequencies.

In linear FDTD, we consider the dielectric constants of Si and SiO_2 as 12 and 2.1, respectively. Noting that the thickness of the graphene ($d_g = 0.34$ nm) is much smaller than the mesh size in FDTD simulation ($0.02a$), we consider the graphene and silicon around it (with a thickness equal to one mesh size) as a composite layer with an equivalent dielectric constant as [29, 30]:

$$\varepsilon_c = \varepsilon_d + i \frac{\sigma_0}{\omega \varepsilon_0 d_g} \rho, \quad (1)$$

where ε_d is the dielectric constant of Si, $\sigma_0 = 6.08 \times 10^{-5} \Omega$ is the initial conductivity of the graphene, and ρ is the filling factor of the graphene inside the composite layer. Under the illumination of an input wave, the increment of the equivalent dielectric constant of the composite layer is calculated as:

$$\Delta \varepsilon_c = \rho \Delta \varepsilon_g, \quad (2)$$

where $\Delta \varepsilon_g = \Delta(n_g^2)$ is the increment of the dielectric constant of graphene. Here n_g is the refractive index of graphene.

In nonlinear FDTD simulations, in order to design high frequency modulators, it is necessary to consider the response time of nonlinear refractive index of graphene. For this purpose, the graphene refractive index increment (Δn_g) is calculated by the following equation:

$$\frac{d}{dt} \Delta n_g = \frac{\beta n_2 I}{\tau_c} - \frac{\Delta n_g}{\tau_c}, \quad (3)$$

where $\tau_c = 100$ fs [28] is the fall time of the refractive index change, $\beta = 1/(1 + I/I_s)$, $n_2 = 10^{-7}$ cm²/W, and $I_s = 600$ MW/cm² [31]. Furthermore, considering that there exists negative absorption nonlinearity of graphene that leads to reduction of its absorption with increasing light intensity, and considering the small effect of absorption of a single layer of graphene in sub-nanometer thickness, we neglect the effect of absorption nonlinearity and only consider Kerr nonlinearity of the graphene similar to our previous work [27].

Results and discussions

The calculation result for the transmission coefficient for the PhC without graphene is shown in Fig. 2. As can be seen, even at high frequencies there are some frequency regions that the transmission is good. In fact, in spite of common opinion, at high normalized frequencies (where photonic bands are above the light line) there are some frequency regions in which the out-of-plane loss is relatively low although it cannot be zero, so one can use these bands to design efficient (high transmission) devices. This is an important point because higher bands can provide photonic modes with higher sensitivity to the change of refractive index. Thus, we study the effect of refractive index of the graphene (due to Kerr nonlinearity) in the PhC at all of the bandgap edges up to the seventh band.

In order to study the effect of graphene on the transmission coefficient at each bandgap edge and to avoid complexity due to the dispersion of graphene, we calculate the transmission coefficient at each selected region of frequency separately with suitable lattice period (for operation wavelength of $\lambda = 1550$ nm). In Fig. 3, the transmission coefficient for PhC with various numbers (N) of graphene layers from 0 to 10 corresponds to the frequency region near the upper side of seventh bandgap. As can be seen, the absorption of graphene leads to reduction of the sharpness of the bandgap edge, resulting reductions in light intensity enhancement and sensitivity of the PhC to the refractive index change. Thus, to achieve lower absorption and stronger light resonance we choose using a single layer of graphene in sub-nanometer thickness.

Through nonlinear FDTD simulations, the PhC output power versus time for a number of fixed incident light intensities for three normalized frequencies near the edge of the seventh bandgap has been plotted in Fig. 4. In Fig. 4, the normalized frequencies are as $f = f_0 - df$, where $f_0 = 1.1383$ corresponds to

the maximum transmission coefficient at the seventh bandgap edge as shown in Fig. 3 and $df = 0, 0.001$ and 0.002 , respectively.

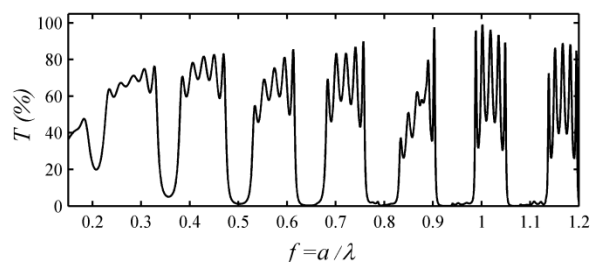


Fig. 2. The transmission coefficient without graphene versus normalized frequency ($f = a/\lambda$).

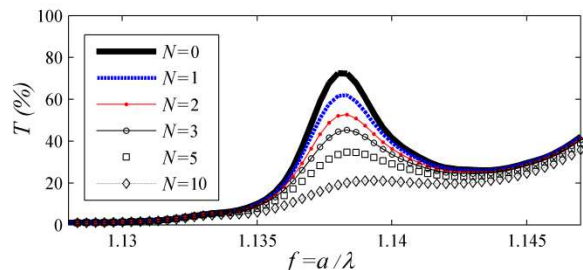


Fig. 3. The transmission coefficient for various number of graphene layers (N) for the normalized frequencies around the edge of seventh bandgap.

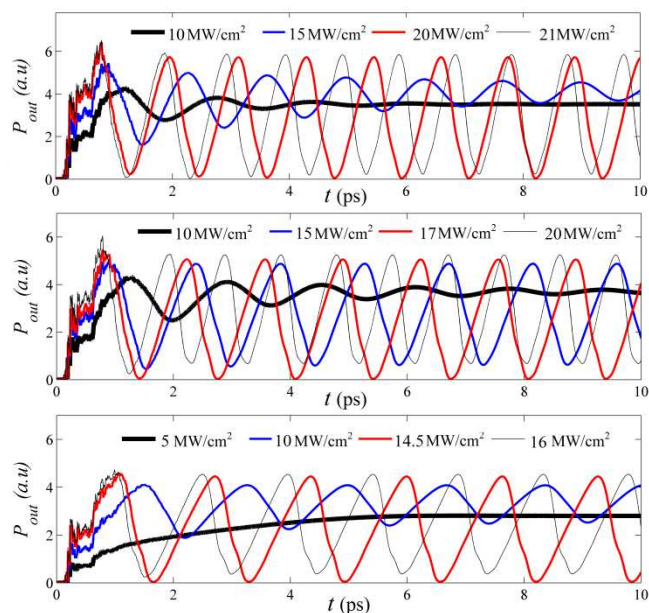


Fig. 4. The transmission power versus time for a number of fixed average intensities of the incidence beam at the normalized frequencies at the seventh bandgap edge for normalized frequencies of $f = f_0 - df$ with $f_0 = 1.1383$ (edge of seventh band gap) and $df = 0$ (up), $df = 0.001$ (middle) and $df = 0.002$ (down).

As can be seen from Fig. 4, self-amplitude modulation takes place with increasing intensity of the input light. At lower light intensities, however, the oscillation is not permanent. By further increasing the input light intensity, permanent oscillation takes place. At a specific input intensity (threshold intensity), the transmission power is oscillated regularly with maximum modulation factor over 97%. By further increasing

the input light intensity (in comparison the threshold intensity), the modulation factor decreases. In addition, as can be seen, with the change of normalized frequency for the transmission peak at the bandgap edge, the threshold intensity and corresponding modulation frequency (with maximum modulation factor) change. This effect is shown in Fig. 5. As can be seen, for normalized-frequency detuning of $df = 0.002$, from the maximum transmission at the bandgap edge ($f_0 = 1.1383$) which is equivalent to tuning of wavelength about 2.7 nm at the wavelength of 1550 nm, the threshold intensity (I_t) frequency decreases from 20 MW/cm² to 14.4 MW/cm² and the modulation frequency (F_M) also decreases from about 0.85 THz to 0.6 THz, respectively.

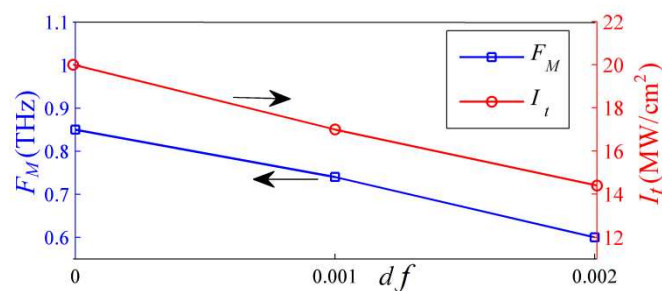


Fig. 5. The modulation frequency (F_M), and threshold intensity (I_t) versus normalized frequency detuning (df) from the edge of seventh bandgap with normalized frequency of $f_0 = 1.1383$.

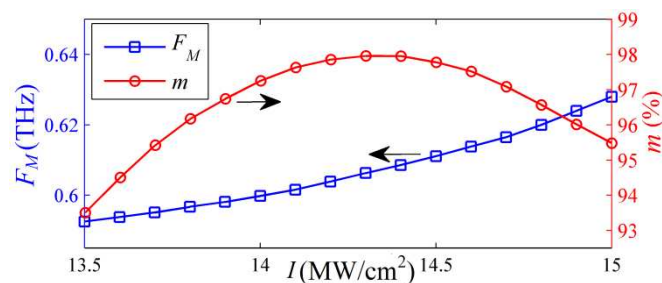


Fig. 6. The modulation frequency (F_M), and Modulation factor (m) versus average intensity of the incidence beam around the threshold intensity with maximum modulation factor for normalized frequency of $f = f_0 - df$ with $f_0 = 1.1383$ (edge of seventh bandgap) and $df = 0.002$.

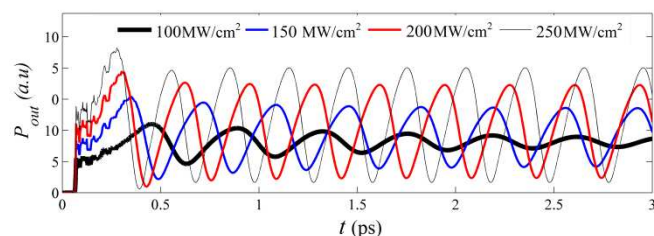


Fig. 7. The transmission power versus time for a number of fixed average intensities of the incidence beam at the normalized frequency of $f = 0.527$ at the third bandgap edge.

Also, another interesting effect is that, in addition to tuning the modulation frequency by changing the input wavelength (Fig. 5), one can also tune the modulation frequency by varying the input intensity with the same high modulation factor. To study this ability in more details, the influence of input intensity

around the threshold intensity (I_t) on the modulation frequency (F_M) and modulation factor (m) is shown in Fig. 6 for the case of normalized frequency detuning of $df = 0.002$ from the seventh bandgap edge. As can be seen from Fig. 6, for input intensity in the range of 13.5 to 15 MW/cm², the modulation frequency can be tuned from about 0.59 to 0.63 THz with the modulation factor keeping higher than about 93%. This means that at the intensities around the threshold intensity (the intensity with maximum modulation depth) the sensitivity of the modulation frequency to the input intensity can be calculated as $dF_M/dI \approx 0.04$ THz/(MW/cm²).

The observed oscillation can be explained by considering four factors, including 1—change of the refractive index of graphene with intensity (due to Kerr effect on graphene), 2—sensitivity of the PhC response to the change of refractive index, 3—nonlinear response time of the graphene (fall time), and 4—response time of the PhC cavity, which is characterized by the quality factor of the cavity.

In detail, the mechanism of the self-modulation can be described as follows. A finite-size PhC can have many intrinsic resonant modes, as shown in Fig. 2. The resonance frequencies of these intrinsic modes will be changed as the graphene layer gives different refractive index under different power of input waves. For higher input power, the graphene's refractive index goes higher, resulting higher effective refractive index of the finite-size PhC and thus lower frequencies of the intrinsic modes. In the system, the frequency of the input wave is set to be equal to the frequency of an intrinsic mode at the beginning when the field intensity in the cavity is zero. Then we can view the following process: At first, the field in the cavity is 0 or very weak, no nonlinear effect exists; after a time period of building up of field in the cavity due to non-zero quality factor of the cavity (or none zero response time of the PhC), the field in the cavity reaches a high value and then nonlinear effects take place, resulting detuning of the cavity, i.e., the field in the cavity decreases; then after some time, the field in the cavity decreases to be very weak. Obviously, such a process would repeat in the system. Such a repeated process accounts for the self modulation phenomenon in the proposed structure. The self modulation period is just about the summation of the building up time and the life time of the resonance mode in the cavity.

From the description of the mechanism, we can see that the modulation frequency is mainly decided by the changing speed of intensity in the PhC, which is related to the quality factor of the intrinsic mode of the PhC. This is reasonable, as the fall time of the graphene is about 100 fs or 0.1 ps, which is much less than the period of the modulation wave. For a further study, in Fig. 7 the result of self-amplitude modulation for a lower bandgap edge (third bandgap) corresponds to the normal frequency of $f = 0.527$ has been shown. As can be seen, in this case, regular oscillation takes place at much higher threshold intensity of more than 200 MW/cm² that is one order of magnitude greater than that obtained for the 7th bandgap edge. However, in this case, the modulation frequency increases up to ~ 3 THz, but the modulation factor decreases to about 85%.

We can explain that the modulation frequency for the modes in lower bands is higher than that for the modes in higher bands by noting that lower quality factor corresponds to higher increase speed of field intensity in the PhC and that the quality factors of the intrinsic modes in the lower bands are less than that in the higher bands because the ripples in the higher bands are sharper than that in the lower bands, as can be seen from Fig. 2.

We can also explain that higher threshold intensity is required for self modulation in the lower bands by noting that the modes in the lower bands have less quality factors, corresponding to smaller ratio of the field intensity in the PhC to that of the input wave, i.e., for the same amount of frequency shift of the modes, higher input power is required.

Another difference between the self modulation in lower and higher bands is that in lower bands regular and high modulation factor oscillations take place in wide range of intensity. As can be seen from Fig. 7, the self-modulation works well for input intensity between 150 and 200 MW/cm². However, in the case of using higher bands, as can be seen from Fig.4, the range of input intensity for obtaining regular and high oscillation is much less and is about 1 MW/cm². Such a phenomenon is also a result of the difference of quality factor for the modes in the higher and lower bands. For low quality factor modes, the intensity of the intrinsic modes in the PhC changes slowly with the input intensity, i.e., not so sensitive with it. As a result, the operating range of input intensity for the self modulation in the lower bands is wider than that in the higher bands.

The self modulation is a novel, interesting phenomenon in the nonlinear PhC cavity. In the frequency domain, a self modulated beam is equivalent to a superposition of two coherent beams with different frequency, so that only one input laser beam is required. Therefore, no expensive mode-locking amplifiers are required as that in the generation of THz waves through frequency difference or photonic mixing, decreasing greatly the system complexity and cost.

Finally, for application purposes, here we present further an estimation of the efficiency for the THz wave generator proposed. As can be seen from Fig. 3 (that is for low light intensities or linear condition), the maximum transmittance at the peak of bandgap edge is ~60% for the case of single layer of graphene ($N=1$) in sub-nanometer thickness, but at high light intensities, as we show in our previous study [27] light distribution inside the PhC changes with increasing refractive index of graphene due to self-focusing effect. This effect leads to more out-of-plane loss so the maximum transmittance at the peak of the modulation in the Fig. 3 decreases to ~30%, corresponding to an average power efficiency of conversion of 15%. Considering that only a part of the modulated wave can be converted to be THz wave output due to the conversion efficiency of the PD or PM and the radiation efficiency of the antenna the actual efficiency may be much lower. Even though, we expect that its efficiency can be higher than that in conventional THz wave generators because the nonlinearity of graphene is high and enhanced in the PhC further and because the proposed structure is very compact as its size is in micrometer order.

Conclusions

It has been shown that in spite of the absorption of graphene, using a single layer of graphene in sub-nanometer thickness inside 1-D slab PhCs and using high normalized frequencies at the higher bandgap edges of the 1-D PhCs, one can provide enhanced nonlinearity with small loss to obtain high frequency (~0.6 THz), high modulation factor (~98%), low intensity threshold (~15 Mw/cm²), self intensity modulation. By considering the advantage of easy fabrication process, small size, high modulation factor, without requiring input of two mode-locked light beams of different frequency, and continuous wave operation, the designed device has a good potential for applications in optical integrated circuits as a pulse generator. Also it has been shown that by tuning the

wavelength about 2.7nm or input intensity of 1.5 MW/cm², it is possible to tune the modulation frequency about 0.25 THz and 0.4 THz, respectively.

At last, we point out that the obtained modulation frequency (<1 THz) at the seventh bandgap is limited due to the response time of the PhCs not due to the response time of the graphene, thus by reducing the response time of the PhCs, it is possible to increase the modulation frequency up to one order of magnitude. However, the challenge is that it may need PhCs with lower quality factors that lead to reduction of PhC sensitivity to the change of graphene refractive index and thus higher threshold intensity. Therefore, obtaining higher modulation frequency with lower threshold intensity by using suitable 1-D or 2-D PhCs can be an interested subject for further investigations. Also, using more number of graphene layers can help to decrease the threshold intensity. However optical loss due to the absorption of graphene makes another limitation in the total achievable quality factor as $1/Q=1/Q_G+1/Q_p$, where Q_G is the quality factor due to graphene absorption and Q_p is the quality factor of the PhC (without graphene), so there is a maximum limit for Q_p that depends on the number of graphene layers. Therefore, for desired modulation frequency one can also architect the number of graphene layers instead of adjusting the PhC quality factor of the PhC. Indeed, with the increase in the number of graphene layers, the sharpness of the bandgap edge (or equivalently the quality factor) will decrease due to the increase in the graphene absorption (as shown in Fig. 3). Moreover, the decrease in quality factor would lead to the decrease in the sensitivity of the PhC response to the change of the effective dielectric constant and decrease of light intensity enhancement inside the PhC. On the other hand, increasing the graphene layers will lead to increasing in the changing sensitivity of effective refractive index of the composite layer to the input intensity. Thus, one can find the optimum number of graphene layers that may also depends on the PhC structure. However in this investigation we have shown that the simplest selection of using only one layer of graphene, one dimensional slab PhC and high normalized frequencies or greater PhC lattice constant are suitable enough to obtain low threshold self-modulation at THz frequencies.

Acknowledgements

This work was supported by the NSFC (Grant No.: 61275043, 61171006, 61107049, 60877034), the Guangdong Province NSF (Key project, Grant No.: 8251806001000004) and the Shenzhen Science Bureau (Grant No. 200805, CXB201105050064A).

Notes and references

^a THz Technical Research Center, Shenzhen Key Laboratory of Micro-nano Photonic Information Technology, Key Laboratory of Optoelectronic Device and Systems of Ministry of Education and Guangdong Province, College of Electronic Science and Technology, Shenzhen University, Shenzhen 518060, China.

^b Department of Physics, Faculty of Science, Esfahan University, Esfahan, Iran.

- 1 A. Dobroiu, C. Otani, and K. Kawase, *Measurement Science and Technology*, 2006, **17**, R161.
- 2 J. F. Federici, B. Schulkin, F. Huang, D. Gary, R. Barat, F. Oliveira, and D. Zimdars, *Semicond. Sci. Technol.*, 2005, **20**, S266.
- 3 J. Federici, and L. Moeller, *J. Appl. Phys.*, 2010, **107**, 111101.

- 4 T. Kleine-Ostmann, K. Pierz, G. Hein, P. Dawson, and M. Koch, *Electron. Lett.*, 2004, **40**, 124.
- 5 P. Zhao, S. Ragam, Y. J. Ding, and I. B. Zotova, *Appl. Phys. Lett.*, 2012, **101**, 021107.
- 6 S. Ragam, T. Tanabe, K. Saito, Y. Oyama, and J. Nishizawa, *J. Lightwave Technol.*, 2009, **27**, 3057.
- 7 T. J. Edwards, D. Walsh, M. B. Spurr, C. F. Rae, M. H. Dunn, and P. G. Browne, *Opt. Express.*, 2006, **14**, 1582.
- 8 R. Sowade, I. Breunig, I. a. Mayorga, J. Kiessling, C. Tulea, Volkmar Dierolf, and Karsten Buse, *Opt. Express.*, 2009, **17**, 22303.
- 9 F. Kadlec, P. Kuzel, and J. L. Coutaz, *Opt. Lett.*, 2005, **30**, 1402.
- 10 R. Kohler, A. Tredicucci, F. Beltram, H. E. Beere, E. H. Linfield, A. G. Davies, D. A. Ritchie, R. C. Iotti, and F. Rossi, *Nature*, 2002, **417**, 156.
- 11 S. Kumar, B. S. Williams, S. Kohen, Q. Hu, and J. L. Reno, *Appl. Phys. Lett.*, 2004, **84**, 2494.
- 12 B. S. Williams, S. Kumar, Q. Hu, and J. L. Reno, *Opt. Express*, 2005, **13**, 3331.
- 13 A. W. M. Lee, Q. Qin, S. Kumar, B. S. Williams, Q. Hu, and J. L. Reno, *Opt. Lett.*, 2007, **32**, 2840.
- 14 D. G. Paveliev, Y. I. Koshurinov, A. S. Ivanov, A. N. Panin, V. L. Vax, V. I. Gavrilenko, A. V. Antonov, V. M. Ustinov, and A. E. Zhukov, *Semiconductors*, 2012, **46**, 121.
- 15 A. Maestrini, J. S. Ward, J. J. Gill, C. Lee, B. Thomas, R. H. Lin, G. Chattopadhyay, and I. Mehdi, *IEEE Trans. Microw. Theory Tech.*, 2010, **58**, 1925.
- 16 L. Li, L. A. Yang, J. C. Zhang, J. S. Xue, S. R. Xu, L. Lv, Y. Hao, and M. T. Niu, *Appl. Phys. Lett.*, **100**, 072104, 2012.
- 17 L. A. Yang, Y. Hao, Q. Yao, and J. Zhang, *IEEE Trans. Electron Devices*, 2011, **58**, 1076.
- 18 B. A. Knyazev, G. N. Kulipanov, and N. A. Vinokurov, *Meas. Sci. Technol.*, 2010, **21**, 054017.
- 19 S. Preu, G. H. Dohler, S. Malzer, L. J. Wang, and A. C. Gossard, *J. Appl. Phys.*, 2011, **109**, 061301.
- 20 E. Rouvalis, C. C. Renaud, D. G. Moodie, M. J. Robertson, and A. Seeds, *Opt. Express*, 2010, **18**, 11105.
- 21 B. Ferguson, and X. C. Zhang, *nature materials*, 2002, **1**, 26.
- 22 M. Tonouchi, *Nature Photonics*, 2007, **1**, 97.
- 23 A. Maestrini, B. Thomas, H. Wang, C. Jung, J. Treuttel, Y. Jin, G. Chattopadhyay, I. Mehdi, and G. Beaudin, *Comptes Rendus. Physique*, 2010, **11**, 480.
- 24 Z. Zheng, C. Zhao, S. Lu, Y. Chen, Y. Li, H. Zhang, and S. Wen, *Opt. Express*, 2012, **20**, 23201.
- 25 Z. B. Liu, X. L. Zhang, X. Q. Yan, Y. S. Chen, J. G. Tian, *Chin. Sci. Bull.*, 2012, **57**, 2971.
- 26 G. Q. Xie, J. Ma, P. Lv, W. L. Gao, P. Yuan, L. J. Qian, H. H. Yu, H. J. Zhang, J. Y. Wang, and D. Y. Tang, *Opt. Mater. Express*, 2012, **2**, 878.
- 27 R. Asadi, Z. Ouyang, Q. Yu, and S. Ruan, *Opt. Express*, 2014, **22**, 14840.
- 28 M. Breusing, C. Ropers, and T. Elsaesser, *Phys. Rev. Lett.*, 2009, **102**, 086809.
- 29 L.A. Falkovsky, *Journal of Physics: Conference Series*, **129**, 012004, 2008.
- 30 M. A. K. Othman, C. Guclu, and F. Capolino, *J. Nanophotonics*, **7**, 2013, 073089.
- 31 H. Zhang, S. Virally, Q. Bao, K. P. Loh, S. M., Ni. Godbout, and P. Kockaert, *Opt. Lett.*, 2012, **37**, 1856.